Journal of The Electrochemical Society, **150** (4) G240-G243 (2003)
0013-4651/2003/150(4)/G240/4/$7.00 © The Electrochemical Society, Inc.

Characterization of SiGe Quantum Dots on SiO_2 and HfO_2 Grown by Rapid Thermal Chemical Deposition for Nanoelectronic Devices

Dong-Won Kim,[a,z] Sungbo Hwang,[b] Thomas F. Edgar,[b] and Sanjay Banerjee[a,*]

[a]*Microelectronics Research Center and* [b]*Department of Chemical Engineering, The University of Texas at Austin, Austin, Texas 78712, USA*

Silicon-germanium quantum dot growth between 500 and 525°C using a $Si_2H_6/GeH_4/H_2$-based chemistry was studied. The nucleation and growth of the SiGe dots were quantified by measuring the nuclei density and the concentration of Ge on SiO_2 and HfO_2 using scanning electron microscopy and atomic force microscopy. The effect of GeH_4 and Si_2H_6 pretreatment on the SiO_2 surface was investigated. It was found that Si atoms dominate the formation of the critical nuclei and Ge atoms impinge on these Si atoms to grow the SiGe dots. The Si atoms that terminate defect sites on SiO_2 and the Si_2H_6 partial pressure determine the densities of SiGe dots. The growth of SiGe dots is limited by the GeH_4 partial pressure, which reduces the activation energy of disilane decompositions in the surface-reaction-limited regime and desorption sites of H from the substrate.
 [DOI: 10.1149/1.1556597]

Manuscript submitted June 5, 2002; revised manuscript received October 18, 2002. Available electronically February 28, 2003.

Silicon (Si) or silicon-germanium (SiGe) dots embedded in an insulator have potential applications for room temperature operation of single-electron transistor memories and nonvolatile memory devices.[1-4] For nonvolatile memory devices, a long retention time at room temperature is essential. In conventional nonvolatile memory devices, further scaling of cells is problematic because of the trade-off between the thickness of the tunneling oxide and the charge retention time. Embedding Si dots on an insulator structure has been proposed to overcome these problems.[5] Several groups have recently implemented charge storage in Si quantum dots. These devices directly tunnel charges through a thin oxide into and out off the Si dots.[6-8] In contrast to Si dots, embedding Ge[9] or SiGe dots in SiO_2 result in longer retention times,[10] because the bandedge of SiGe dots is lower than that of Si. It is also necessary to have a high dot density to fabricate a single electron transistor and to sustain a long retention time in nonvolatile memory devices.[5,7]

Recent research on alternate gate dielectric materials to replace silicon dioxide in standard complementary metal oxide semiconductor (CMOS) technology has focused on materials such as high-*k* gate dielectrics, which have higher dielectric constant (ε) values that provide low equivalent oxide thickness (EOT) gates while allowing a thicker film for reduced gate leakage, improved resistance to boron diffusion, and better reliability characteristics.[11-13]

In this study, we present a comparative study of the nucleation and growth of SiGe self-assembled quantum dots (SAQDs) on SiO_2 and on a high-*k* dielectric, HfO_2, which is suitable for tunneling oxides (3 nm) in memory devices fabricated using rapid thermal chemical vapor deposition (RTCVD) at low temperature (500-525°C). SiGe dot parameters such as dot height, radius, and density were compared for various Si_2H_6/GeH_4 gas ratios and processing temperatures on different dielectric substrates.

Experimental

The flash memory structures were fabricated on p-type (100) silicon wafers using local oxidation of silicon isolation with field oxide thickness of 360 nm. After definition of the active area and pregate cleaning (a standard RCA clean and dilute HF etch), prior to deposition of the SiO_2 and HfO_2 insulator films, the wafers were immersed in a diluted HF solution to remove native oxide and loaded directly into the furnace or sputtering chamber for deposition of SiO_2 or HfO_2 dielectric films, respectively.

The HfO_2 was produced by first sputtering Hf metal and annealing. About a 4-5 nm thick Hf metal was first deposited by dc magnetron sputtering technique at a base pressure of $\sim 10^{-7}$ Torr. The Ar gas flow rate and the gas pressure were 20 standard cubic centimeters per minute and 30 mTorr, respectively. The dc power was as low as 200 W to reduce sputtering damage. The sputtered Hf metal was annealed at 600°C for 40 s in a N_2 atmosphere by using a rapid thermal process. Annealing the metallic Hf film resulted in a 4.2 nm thick film. The 3.8 nm thick SiO_2 films were thermally grown at 750°C for 5 min in an O_2 atmosphere. On these dielectric film substrates, the SiGe dots were grown in a RTCVD chamber (base pressure of 7×10^{-7} Torr) using high purity GeH_4 gas and Si_2H_6 at temperatures of 500-525°C, at 5°C intervals. The growth time was varied from 60 to 300 s. The chamber pressure during growth was 600 mTorr. Before the nuclei were formed, the samples were exposed to a Si_2H_6 or GeH_4 for 10 to 20 s at a temperature of 520°C. These samples were studied with atomic force microscopy (AFM), field emission scanning electron microscopy (FE-SEM), Auger electron spectroscopy (AES), and X-ray diffraction (XRD) to characterize the SiGe dots and the concentration of Ge in SiGe dots and the films, respectively. This paper focuses on the characterization of the self assembled quantum dots; the electric device results will be presented later.

Results and Discussion

Figure 1 shows AFM images of self-assembled SiGe dots on HfO_2 and SiO_2. The surface roughness of the dielectric substrates before growing SiGe dots is less than 1 nm measured by AFM, as shown in Fig. 1c, HfO_2, and 1d, SiO_2. Smooth surface regions (root mean square roughness <1 nm) are the dielectric substrates without dots; the rough surface morphologies indicate the existence of SiGe dots. For an estimation of the incubation time, which is the time when the first stable SiGe dots form, Fig. 2 shows SEM images of dots deposited using various growth times at 520°C with 0.75 gas ratio of GeH_4 to Si_2H_6 on the SiO_2 substrate. From Fig. 2a, the incubation times seem to be approximately between 60 and 90 s. SiGe dots start coalescence into continuous films which is evident from the merging of the dots, changing the shape of the dots around 180 s. At low temperatures, adatoms that arrive on the substrate formed a stick and are stationary because of the lack of sufficient thermal energy to cause desorption or diffusion. At high temperatures, the energy to desorb adatoms is large so that adatoms desorb from surface or diffuse to neighboring nuclei. Figure 3 shows the dependence of SiGe dot density on time and substrate temperature at fixed gas ratio of GeH_4 to Si_2H_6 on SiO_2 and HfO_2, respectively. The stable dot density is observed to increase approximately linearly with deposition time and then saturate at around 10^{11} cm^{-2} depending on substrate and process temperature. These values agree with

* Electrochemical Society Active Member.
z E-mail: timokim@mail.utexas.edu

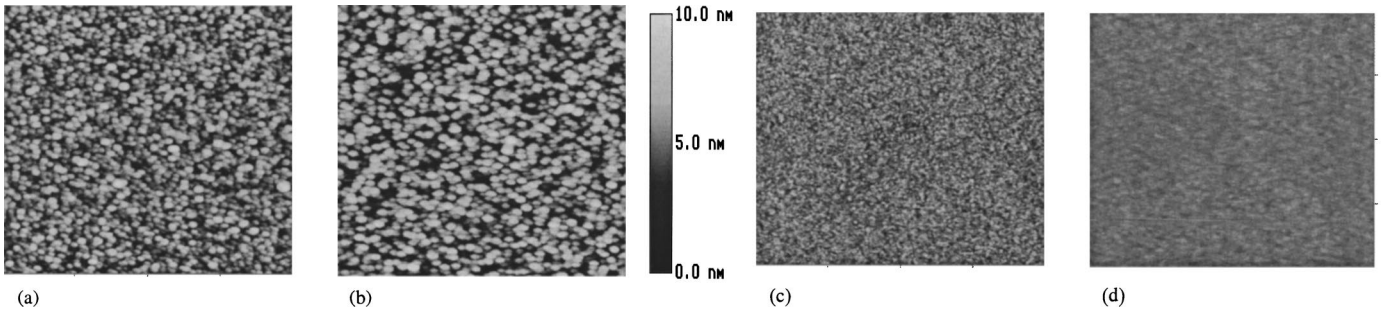

Figure 1. AFM scan images (1×1 μm) showing the self-assembled SiGe dots on (a) HfO_2 and (b) SiO_2 at 510 and 525°C respectively, for 90 s with 0.75 gas ratio of GeH_4 to Si_2H_6. The vertical scale of the image is 10 nm, with white representing the highest point and black the lowest point in the images.

nucleus saturation densities of 10^9-10^{12} cm^{-2} reported in the literature for various conditions.[14-15] The dot density decreases due to dot coalescence for longer time. The nuclei density data show that there is weak dependence on the substrate temperature. It is well known that the nucleation rate depends on how many nuclei of critical size form on a substrate; that these nuclei can grow through direct impingement of atoms from the gas phase.[14] However, the rate of growth of the critical nuclei depends on the rate at which impinging adatoms attach to it. The reason for the different trend in dot density at different temperatures is that the Si and Ge adsorption rate on the surface at same total reactant flow rate is more a dominant factor than the surface condition of the substrate in the temperature range from 515 to 525°C.

Table I shows the summary of dot parameters grown at various temperatures with a fixed gas ratio of GeH_4 and Si_2H_6 on SiO_2 and HfO_2 substrate, analyzed by AFM. The maximum height, radius, and density of the dots are observed at 515 and 520°C on HfO_2 and SiO_2 substrates, respectively. On a SiO_2 substrate, the radius of a typical dot is a maximum at 515°C due to the wetting layer on the surface and low density of dots at low temperature. The average shape (defined here as height-to-radius ratio) increases as the temperature increases, meaning the dot has faster vertical growth with increased temperature. The SiO_2 substrate changes the average shape from a ratio of 0.18 to 0.45 as temperature increases. By contrast, the HfO_2 substrate changes in average shape from 0.8 to 0.55. The change in average shape at different temperatures indicates that the SiGe growth temperature affects the SiGe dot shape whether the substrate is SiO_2 or HfO_2. However, a transition temperature for height and density of these quantum dots was obtained on SiO_2 and HfO_2 surfaces at 520 and 515°C, respectively.

To determine the influence of the GeH_4 partial pressure on SiGe dot nucleation growth was studied at fixed total gas flow before the coalescence of dots occurred. Figure 4 shows the summary of the SiGe dot density deposited on SiO_2 and HfO_2 substrates at a temperature of 520 and 510°C *vs.* gas ratio of GeH_4 to Si_2H_6. The influence of GeH_4 partial pressure on the SiGe dot density and maximum density of dots are similar irrespective of whether the nucleation takes place on a SiO_2 or HfO_2 substrate. SiGe dots did not form when only GeH_4 or Si_2H_6 gas was flowed. SiGe dots density increases as the gas flow ratio of GeH_4 to Si_2H_6 increases. However, at a gas flow ratio of GeH_4 to Si_2H_6 of 0.75, a maximum dot density is observed on SiO_2 and HfO_2 substrates. For the gas ratios between 0.75 and 1, the SiGe dot density decreases with an increase of the gas ratio of GeH_4 to Si_2H_6. It is found that the activation energy of SiGe dot on SiO_2 and HfO_2 substrate in this temperature range is related to the gas flow ratio.[16-17]

To study the early stages of Si and Ge reaction on the SiO_2 substrate, we tested a pretreatment process; Si_2H_4 or GeH_4 alone was flowed before flow of the mixture of Si_2H_6 and GeH_4 gas. Figure 5 shows an AFM image of SiGe dots that were grown for 90 s with 0.75 gas ratio of of GeH_4 to Si_2H_6 after a 20 s pretreatment of Si_2H_6 or GeH_4 at 525°C. The SiGe dot density was 3.5 times higher when using Si_2H_6 pretreatment than without pretreatment and small dots are obtained. With GeH_4 pretreatment, the density of SiGe dot decreased and the size of dot increased compared to without the pretreatment step. Using AES the germanium concentration of SiGe quantum dots on the tunneling dielectrics has been tested. From comparing Ge concentration for 10 and 20 s pretreatment of Si_2H_6, Ge concentration of the dots for a 20 s Si_2H_6 pretreatment sample is approximately twice that in a 10 s Si_2H_6 pretreatment sample, as shown in Fig. 6. However, the Ge concentration and the density of the dots is shown to be independent of the duration of the GeH_4 pretreatment step before flow the of Si_2H_6 and GeH_4 mixture gas. Furthermore, the density of dots with GeH_4 gas pretreatment is lower than without gas pretreatment.

From experiments by Classsen[18] and Fitch,[19] initial Si nucleation and growth on dielectric substrate such as SiO_2 and Si_3N_4 is mainly determined by hydrogen adsorption and O—H bonds that block adsorption sites for Si atoms. The most likely mechanism involved

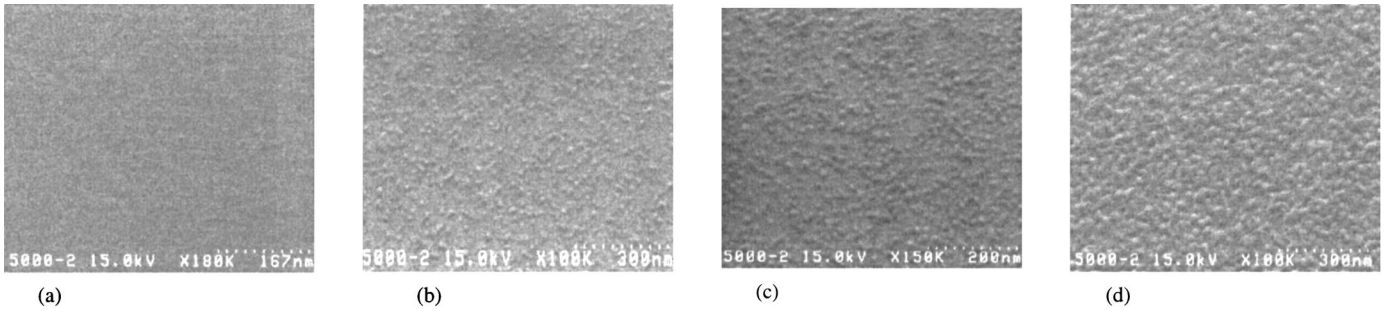

Figure 2. SEM images of dots deposited on the various growth times: (a) 60 s, (b) 90 s, (c) 120 s, and (d) 180 s at 520°C with 0.75 gas ratio of GeH_4 to Si_2H_6 on SiO_2 substrate.

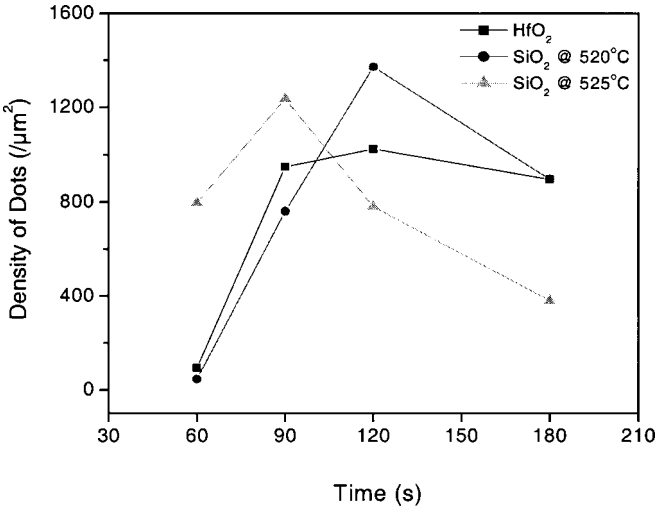

Figure 3. Dependence of density of dots on time and substrate temperature.

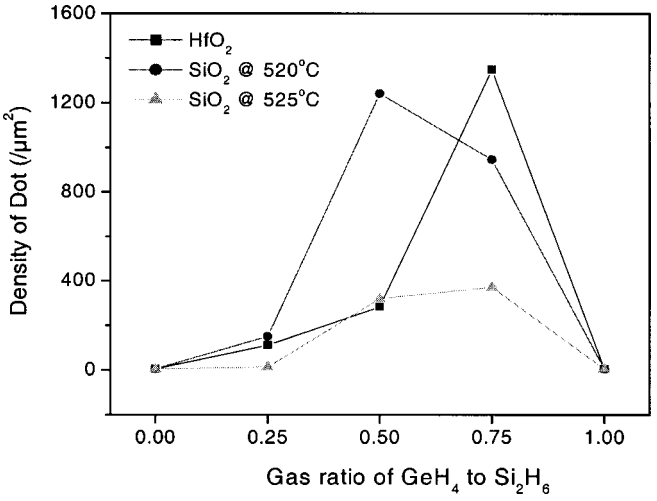

Figure 4. Summary of the SiGe dot density deposited on SiO_2 and HfO_2 substrates at the fixed temperatures *vs.* gas ratio of GeH_4 to Si_2H_6.

in SiGe growth on the Si surface has been described by Malik *et al.*[16] by following the reaction

$$Si_2H_6(g) + 2* \rightarrow 2SiH_3(s) + nGe(s) \rightarrow 2Si(s) \quad [1]$$

$$GeH_4(g) + * \rightarrow GeH_4(s) \rightarrow Ge(s) \quad [2]$$

where * is the vacant site of on the surface and n is a constant. Since the Ge-H bond[20] is a weaker bond than Si-H, [21] passivated H on Ge atoms at the substrate surface is thermodynamically more likely to dissociate, and Ge surface atoms serve as doubly occupied dimers to recombine with surface H atoms.[22] Ge atoms are perhaps the main desorption sites of H, hence the adsorbed species migrate to the Ge sites.[23] Therefore, the effect of GeH_4 pretreatment is that Ge atoms easily generate the vacant sites due to the weaker bond between Ge and H. Most of the vacant sites are terminated by Ge atoms. The enhancement of dot density with Si_2H_6 pretreatment can be explained by the accelerated adsorption rate of Si atoms on the substrate during Si_2H_6 pretreatment. From Fig. 4 and 6, it is found that impinging Si atoms on a surface-limited site with Si_2H_4 gas pretreatment and then impinging Ge on the Si nucleus can cause nucleation growth. However, Ge could not make critical nucleation size during the GeH_4 gas pretreatment, which reduces the surface limited sites so that Si atoms after the Ge burst nucleate at limited sites. The dot density is reduced and dot size increases due to sufficient Ge sources. More Ge atoms are incorporated into the growing SiGe dots because of the higher reactivity of Si_2H_6. The Si_2H_6 gas has a higher decomposition rate than GeH_4 at low temperatures below 600°C, which leads to the low concentration of Ge and higher incorporation rate of Si atoms. Si_2H_6 and GeH_4 can be decomposed in the temperature range of 480-545°C, and in this range, the Ge fraction in the film is mainly determined by GeH_4 partial pressure and stabilized in a fixed gas flow rate of germane to total reactant gas. The growth of quantum dots is then determined by Si and Ge rate arrival, be it via direct impingement or by surface diffusion, to an existing dot. Where the atom attaches to existing dots and determines the dot shape, the location of attachment in turn depends upon the pressure and temperature range of the process.

Figure 7 shows the relationship between dot size (before the coalescence) formed on SiO_2 and the thickness of layers on the Si substrate for the same process conditions in the temperature range of 500 to 530°C. XRD analyzed the thickness of SiGe film on Si. The dot size formed on SiO_2 is in proportion to the thickness of layers grown on Si. The dot size is about half as thick as layers on silicon until the dots coalesce. The size of dots formed at a higher temperature (530°C) with a higher than 0.75 gas ratio of GeH_4 to Si_2H_6, where the dots coalesce rapidly, is the same as the thickness of layers grown on Si. Since the characteristics are the same as the growth rate of the silicon-germanium epitaxial layer, the control of dot size can be based on the growth rate.

Conclusion

In this study, we present a comparative study of the nucleation and growth of SiGe quantum dots on SiO_2 and on a high-*k* dielectric, HfO_2, which are suitable for tunneling oxides (3 nm) in flash memory devices fabricated using RTCVD at low temperature (500-525°C). SiGe dot parameters such as dot height, radius, and density were compared for different Si_2H_6/GeH_4 gas ratios, processing temperatures, and times on different dielectric substrates. We found that the size and rate of the formation of the critical nuclei depend upon the Si reactant concentrations. The Ge reactant concentrations affect the height and size of the dots as impinging Ge atoms attach to

Table I. (a) Height and (b) average radius of SiGe dots on SiO_2 and HfO_2 substrates *vs.* temperature.

	510°C		515°C		520°C		525°C	
Dot parameter	HfO_2	SiO_2	HfO_2	SiO_2	HfO_2	SiO_2	HfO_2	SiO_2
Density (μm^{-2})	415	70	1024	210	792	946	694	371
Diameter (nm)	6.4	5	5.3	19	8	16.8	7.2	7.8
Average height (nm)	3.8	3.5	4.2	3.5	4.0	3.8	3.85	3.5
Average shape (Height/radius)	0.55	0.7	0.8	0.18	0.5	0.22	0.53	0.45

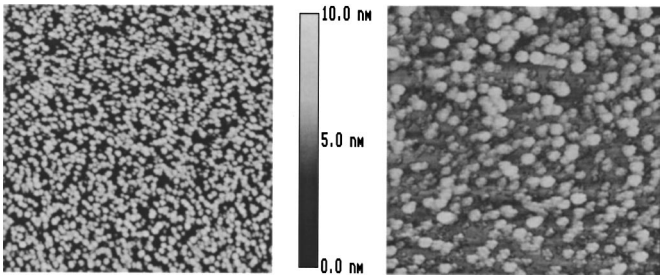

Figure 5. AFM image of the SiGe dots for 90 s with 0.75 gas ratio of GeH_4 to Si_2H_6 after the 20 s pretreatment step of different gases, (a) Si_2H_6 or (b) GeH_4 at 525°C, respectively.

critical Si nuclei. As the ratio of Si_2H_6 to GeH_4 decreases, the height of nuclei and the concentration of Ge in dots increase. We have also demonstrated that the SiGe dot shape is affected by the SiGe growth temperature, but is independent of whether the substrate is SiO_2 or HfO_2. It was also found that the Ge atoms were the main desorption sites of H from the substrate, creating sites presumably involved in the adsorption and decomposition of Si_2H_6 because of the weaker bond between Ge and H. Hence, the Si species migrate to the Ge sites. The Si_2H_6 pretreatment process is a useful method to increase density of dots for nanoelectronic device fabrication.

Acknowledgments

This work was supported in part by the MARCO-Focus Center on MSD, Semiconductor Research Corporation and TATRP.

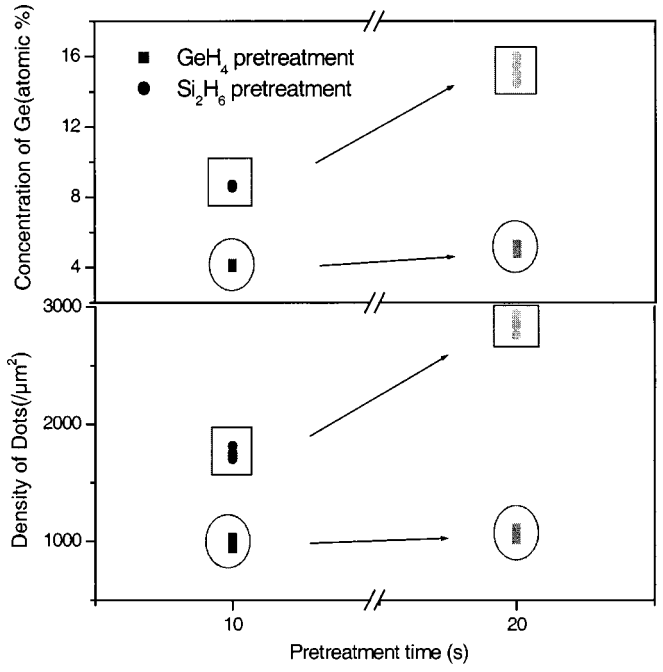

Figure 6. Comparison of Ge content in the SiGe dot *vs.* the density of dots after 10 and 20 s bursting of Si_2H_6, and GeH_4, respectively.

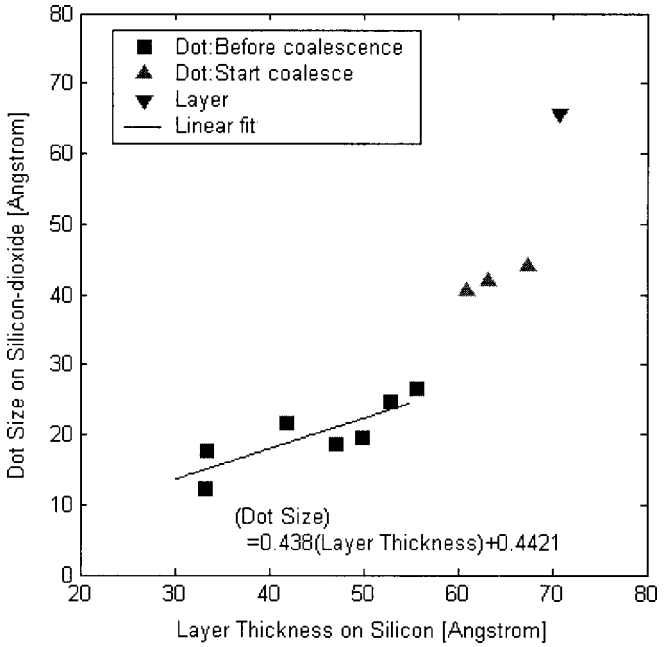

Figure 7. Relationship between dot size (before coalescence) formed on SiO_2 and the thickness of layers on the Si substrate at the same process conditions in the temperature range of 500-530°C.

The University of Texas at Austin assisted in meeting the publication costs of this article.

References

1. A. Nakajima, T. Futatsugi, K. Kosemura, T. Fukano, and N. Yokoyama, *Appl. Phys. Lett.*, **70**, 1742 (1997).
2. L. Guo, E. Leobandung, and S. Y. Chou, *Appl. Phys. Lett.*, **70**, 850 (1997).
3. K. Yano, T. Ishii, T. Hashimoto, T. Kobayashi, F. Murai, and K. Seki, *IEEE Trans. Electron Devices*, **41**, 1628 (1994).
4. Y. Takahashi, M. Nagase, H. Namatsu, K. Kurihara, K. Iwadate, Y. Nakajima, S. Horiguchi, K. Murase, and M. Tabe, *Tech. Dig. - Int. Electron Devices Meet.*, **1994**, 938.
5. H. I. Hanafi, S. Tiwari, and I. Khan, *IEEE Trans. Electron Devices*, **43**, 1553 (1996).
6. I. Kim, H. Han, H. Kim, J. Lee, B. Choi, S. Hwang, D. Ahn, and H. Shin, in *Proceedings of the International Electron Devices Meeting*, IEEE, Vol. 98, p. 111 (1998).
7. S. Tiwari, F. Rana, H. Hanafi, A. Hartstein, E. Crabbé, and K. Chan, *Appl. Phys. Lett.*, **68**, 1377 (1995).
8. Y. Shi, K. Saito, H. Ishikuro, and T. Hiramoto, *J. Appl. Phys.*, **84**, 2358 (1998).
9. D. W. Kim, Y. H. Kim, X. Chen, C. H. Lee, S. C. Song, F. Prins, D. L. Kwong, and S. Banerjee, *J. Vac. Sci. Technol. B*, **19**, 1104 (2001).
10. Y.-C. King, T.-J. King, and C. Hu, *Tech. Dig. - Int. Electron Devices Meet.*, **1998**, 115.
11. G. D. Wilk, R. M. Wallace, and J. M. Anthony, *J. Appl. Phys.*, **87**, 484 (2000).
12. K. Onishi, L. Kang, R. Choi, E. Dharmarajan, S. Gopalan, Y. Jeon, C. S. Kang, B. H. Lee, R. Nieh, and J. C. Lee, Technical Digest for VLSI Symposium, p. 131 (2001).
13. L. Kang, K. Onishi, Y. Jeon, B. H. Lee, C. Kang, W.-J. Qi, R. Nieh, S. Gopalan, R. Choi, and J. C. Lee, *Tech. Dig. - Int. Electron Devices Meet.*, **2000**, 35.
14. M. Ohring, *The Materials Science of Thin Films*, 2nd ed., p. 211, Academic Press, Boston (1992).
15. D. Walton, T. N. Rhodin, and R. W. Rollons, *J. Chem. Phys.*, **38**, 2698 (1963).
16. R. Malik, E. Gulari, S. H. Li, and P. Bhattacharya, *J. Appl. Phys.*, **73**, 5193 (1993).
17. Y. Zhong, M. Öztürk, D. Grider, J. Wortman, and M. Littlejohn, *Appl. Phys. Lett.*, **57**, 2092 (1990).
18. W. A. P. Claassen and J. Bloem, *J. Electrochem. Soc.*, **128**, 1353 (1981).
19. J. T. Fitch, *J. Electrochem. Soc.*, **141**, 1046 (1994).
20. B. Ruscic, M. Schwarz, and J. Berkowitz, *J. Chem. Phys.*, **92**, 1865 (1990).
21. S. Gates and C. Chiang, *Chem. Phys. Lett.*, **184**, 448 (1991).
22. C. Li, S. John, and S. Banerjee, *J. Electron. Mater.*, **24**, 875 (1995).
23. S. A. Campbell, *Mater. Sci. Eng.*, **R20**, 1 (1996).